Energy-Based Aeroelastic Optimisation of a Morphing Wing

R. De Breuker⋆*, M. M. Abdalla*⋆ *and Z. Gürdal*⋆
⋆*Delft University of Technology*
Kluyverweg 1, 2629HS Delft, the Netherlands

Abstract

Due to the often conflicting requirements in an aircraft's mission, designers have to make compromises regarding wing layout leading to sub-optimal performance in individual segments of their mission. Morphing wings are envisioned to enable an aircraft to fly efficient multi-role missions by changing the shape of the wing according to flight conditions. Morphing between various shapes often requires substantial elastic or rigid body shape changes. During these shape changes, the required morphing energy could offset the gain in aerodynamic efficiency. Therefore, an aeroelastic analysis tool for morphing maneuvers is needed. The present paper extends previous work by the authors where large morphing changes are analysed based on nonlinear beam theory coupled to a panel-based lifting line theory. The extended code is used as the basis for an aeroelastic optimisation of a morphing wing. The wing is equipped by an arbitrary number of hinges, and the amount of folding/sweep/twist at each hinge is used as design variable. The aerodynamic performance of the wing, measured by its lift-to-drag ratio, is maximised. It is demonstrated that substantial improvements in aerodynamic performance can be obtained by wing morphing in terms of distributed hinge rotations around the three wing axes.

1. Introduction

Due to the often conflicting requirements on an aircraft's mission (e.g., loiter and high-speed dash) designers have to make trade-offs regarding wing layout which compromises aircraft performance. For each segment of the mission, there exists an ideal shape of the wing for optimal performance, and it is therefore advantageous if the wing can conform to all of these shapes by *morphing* from one to another. Interest in morphing technology has increased substantially over the past decade. The Defense Advanced Research Projects Agency (DARPA) has defined a morphing aircraft as an aircraft that i) changes its state substantially, ii) provides superior system capability and iii) uses a design that integrates innovative technologies.[1]

Considerable effort has been spent on the analysis of morphing structures, including aeroelastic effects. General planform wings with morphing airfoils are considered[2–4] as well as with variable span.[5] Recent work by the authors was also spent of the fast aeroelastic analysis of a morphing wing.[6]

For optimisation studies of morphing wings fast analysis of morphing energy requirements is essential. Actuation power and added weight required to perform morphing manoeuvres are compared to the aerodynamic/performance gains to assess whether overall performance improvement is possible or not. The optimization of morphing wings for improved performance and minimum actuator energy is carried out by Prock *et al.*[7] Other optimization efforts have been carried out in the field of combined span/airfoil optimisation,[8] combined aspect-ratio/sweep optimisation,[9] or optimisation for pull-up manoeuvres.[10]

Optimisation studies related to the structural design of morphing concepts have also been reported in the literature. Topology optimisation of smart actuator placement using genetic algorithms[11] and the topology optimisation of wing skin thicknesses, spar thicknesses, and flap deflections of morphing wings for aeroservoelastic concepts.[12] Multilevel variable fidelity optimisation techniques for morphing structures are also investigated.[13]

An analysis tool for morphing wings that allow morphing to any arbitrary shape in three dimensions while allowing the hinge or flexible locations to be variable and simultaneously taking into account aerodynamics, structural response, and actuation energy, was developed recently by the authors.[6] The current paper focusses on the aeroelastic optimisation of morphing wings. The optimisation routine is a nonlinear constraint optimisation technique. Sensitivity information of the objective function with respect to the design variables is provided to the optimiser to improve efficiency.

The rest of the paper is organised as follows. First, the objectives of the analysis are laid out and the problem precisely formulated. This is followed by sections on the structural model, the aerodynamic model, and the details aeroelastic analysis algorithm. Subsequently the optimisation routine with all of its relevant aspects is dealt with. Finally, results and conclusions are presented.

2. Structural Model

The structural model consists of linear beam elements in a three-dimensional co-rotational framework. The benefit of using such a framework instead of using nonlinear finite elements is the fact that the local rotations of the beam are known, which comes in handy to derive the aerodynamic mesh from the structural one. This facilitates the analysis of aerodynamic forces and moments considerably (see section 3).

The local beam element formulation is a linear shear-flexible element. The beam elements are connected with flexible rotational springs. The local beam element is based on the element of Goyal and Kapania.[14] The element has 22 degrees of freedom and five nodes (four equally-spaced nodes with one additional node in the middle of the beam). The beam allows for shear flexibility and reduces exactly to the standard Hermitian beam element in the limit of high slenderness ratio. The DOFs corresponding to the interior nodes are statically condensed leading to a 12×12 element stiffness matrix. This element has been designed for the modelling of fibre-reinforced laminated composite structures allowing for arbitrary material coupling. As an input, the beam element accepts the full anisotropic 6×6 beam section stiffness matrix. Results from, for instance, the Variational Asymptotical Beam Sectional Analysis (VABS)[15] can be used. VABS calculates the beam section stiffness matrix for an arbitrary 2D composite cross-section giving a fully populated beam stiffness matrix.

The co-rotational approach converts local element forces from the local to global frames. The essential part of the co-rotational formulation is the definition of a local element frame and defining the local element degrees of freedom with respect to that frame. The formulation used in this paper is adopted from Battini and Pacoste.[16]

The global nodal degrees of freedom for the co-rotational element are the displacements of the nodes in the global coordinate system and nodal rotation vectors describing the rotations between the undeformed and deformed configurations.

$$\mathbf{p} = \begin{bmatrix} \mathbf{u}_1^T & \boldsymbol{\theta}_1^T & \mathbf{u}_2^T & \boldsymbol{\theta}_2^T \end{bmatrix}^T . \tag{1}$$

The local degrees of freedom are defined as,

$$\mathbf{p}_\ell = \begin{bmatrix} \bar{u} & \boldsymbol{\vartheta}_1^T & \boldsymbol{\vartheta}_2^T \end{bmatrix}^T \tag{2}$$

where $\bar{u}$ is the change of element length between the current and initial configurations, $\bar{u} = L - L_0$, and the vectors $\boldsymbol{\vartheta}_i$ are the nodal rotation vector resolved in the local element frame.

The global element force vector and tangent stiffness can be obtained from the local element forces and stiffness matrix using the geometrical relation between the local and global degrees of freedom. The local element forces are obtained from the linear relation,

$$\mathbf{f}_\ell = \mathbf{K}_\ell \cdot \mathbf{p}_\ell, \tag{3}$$

while the global element force and tangent stiffness are given by,

$$\mathbf{f} = \mathbf{B}^T \mathbf{f}_\ell, \tag{4}$$

$$\mathbf{K}_t = \mathbf{B}^T \mathbf{K}_\ell \mathbf{B} + \frac{\partial \mathbf{B}}{\partial \mathbf{p}} : \mathbf{f}_\ell. \tag{5}$$

Derivation and expressions for the transformation matrix $\mathbf{B}$ and further details of the element can be found in Battini and Pacoste.[16]

Each beam element is connected to its neighbour via a rotational spring. Thus, each node is split into two overlapping nodes. The two nodes share the same displacement degrees of freedom, but have different rotational degrees of freedom. This yields nine DOFs per node (three displacements and six rotations) per physical node. The two overlapping nodes are connected using a torsional spring (see figure 1). This allows the representation a rigid connection (infinite spring stiffness), a hinge (zero spring stiffness), and semi-flexible hinges (finite value of the spring stiffness). Actuation moments, composing the actuation moment vector $\mathbf{M}_a$, can be applied to each spring location in order attain a desired difference in rotation in any direction.

3. Aerodynamic Model

The prediction of the aerodynamic performance of a wing is a fairly complex problem and can be modelled with any degree of sophistication. For a coupled aeroelastic problem such as a morphing wing, it is important to match the level of modelling of structures and aerodynamics. For the adopted structural model using beam elements, it is reasonable

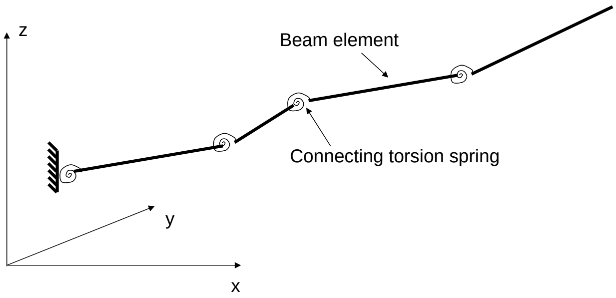

Figure 1: Cantilevered wing built up from hinged beam elements

to use a one-dimensional aerodynamic model such as lifting line theory to predict the aerodynamic loads.[17] When a better aerodynamic model is warranted, two-dimensional panel methods such as the vortex lattice method[12,18] can also be used. A one dimensional vortex-based method is implemented following Katz and Plotkin.[19] The finite wing is represented by a set of n linearly added vortex lines each with strength Γ_i. Flow tangency condition demands zero normal flow on the airfoil and, as such, the unknown vortex strengths are calculated. The lift and induced drag forces are calculated from the vortex strength distribution over the wing. An estimate for the viscous drag is made based on the 2D lift-drag polar. The induced and viscous drag are added to give the total drag. The aerodynamic forces are assumed to act at the quarter chord point of each aerodynamic panel.

The coordinates aerodynamic panels are linked to the structural element geometry. Each structural beam element has an element fixed frame (see figure 2) and the node locations are known as well as the local rotations per node (because of the co-rotational framework). From these parameters, the two-dimensional aerodynamic mesh can be deducted from the one-dimensional beam element. Each beam element can contain multiple aerodynamic panels. In order to achieve this, the nodal rotations are linearly interpolated per beam element.

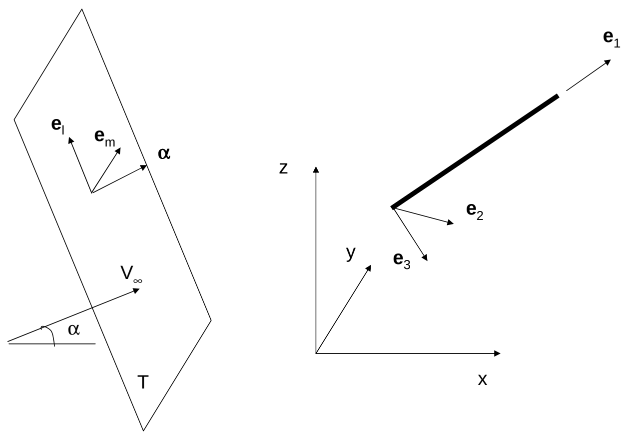

Figure 2: Structural and aerodynamic reference frames

The vector directions of lift, drag and moment forces are linked to the structural element frame. The panel normal is along the direction $\mathbf{e}_3$. The drag force acts along the free-stream velocity vector $\boldsymbol{\alpha}$,

$$\boldsymbol{\alpha} = [\cos(\alpha) \;\; 0 \;\; \sin(\alpha)]^T. \tag{6}$$

where α is the angle of incidence. The direction of the aerodynamic moment vector, $\mathbf{e}_m$, lies in the plane perpendicular to $\boldsymbol{\alpha}$, usually referred to as the Trefftz plane, and is defined as the projection of the element vector $\mathbf{e}_1$ on the Trefftz plane,

$$\mathbf{e}_{1,p} = \mathbf{e}_1 - (\mathbf{e}_1 \cdot \boldsymbol{\alpha}) \cdot \boldsymbol{\alpha} \tag{7}$$

$$\mathbf{e}_m = \frac{\mathbf{e}_{1,p}}{||\mathbf{e}_{1,p}||}. \tag{8}$$

The lift direction, $\mathbf{e}_l$, is perpendicular to both $\boldsymbol{\alpha}$ and $\mathbf{e}_m$,

$$\mathbf{e}_l = \boldsymbol{\alpha} \times \mathbf{e}_m \tag{9}$$

When all the aerodynamic forces and moments are decomposed along their appropriate vectors in the global frame, they are converted to statically equivalent nodal forces to construct the global aerodynamic force vector $\mathbf{f}_a$. The derivative of this aerodynamic force vector with respect to the global degrees-of-freedom $\mathbf{p}$ is the aerodynamic sensitivity matrix $\mathbf{A}$. The latter is obtained by using automatic differentiation.[20]

4. Static Aeroelasticity

In the present study, only static aeroelastic effects are considered. The discrete equilibrium equations are written as,

$$\mathbf{f}(\mathbf{p}) = \mathbf{f}_{ex}(\lambda) + \mathbf{f}_a(\mathbf{p}, \alpha, q) \tag{10}$$

where $\mathbf{f}$ is the vector of internal forces that depend on the vector of global degrees-of-freedom $\mathbf{p}$, $\mathbf{f}_{ex}$ the external forces that depend on a load parameter λ, and $\mathbf{f}_a$ the aerodynamic forces which depend on the degrees-of-freedom $\mathbf{p}$, the angle of incidence α and the dynamic pressure q.

When significant nonlinearities are involved, it is customary to trace the response as function of the load parameter λ. In order to determine the equilibrium position at a certain intermediate value for the control parameter an initial guess $\mathbf{p}_0$ is made for the displacement field (usually using a prediction based on the last converged step), then the exact equilibrium displacements are found using the Newton-Raphson method.[21] An overview of the iteration loops is given in figure 3.

Assume that the dynamic pressure q is the only control parameter, the displacement increment $\Delta\mathbf{p}$ is determined from,

$$\mathbf{J}(\mathbf{p}_0, q)\Delta\mathbf{p} = \mathbf{f}_a((\mathbf{p}_0), q) - \mathbf{f}(\mathbf{p}_0) \tag{11}$$

where $\mathbf{J}$ is the system Jacobian matrix, defined as:

$$\mathbf{J}(\mathbf{p}_0, q) = \mathbf{K}_t(\mathbf{p}_0) - \mathbf{A}(\mathbf{p}_0, q) \tag{12}$$

An analogous incremental equilibrium equation can be derived when the control parameter is other than the dynamic pressure.

To simulate a morphing manoeuvre, the target shape of the wing is described by prescribing the difference in rotations across each spring. The load parameter controls the amplitude of the rotation difference. The incremental equation then becomes,

$$\mathbf{J}\Delta\mathbf{p} = \mathbf{f}_a - \mathbf{f} + \mathbf{f}_c. \tag{13}$$

where $\mathbf{f}_c$ is the actuation moment vector. Since the rotation difference across the nodes is prescribed, this can be treated as a multi-point constraint (MPC) and the actuation moments are recovered as the MPC reactions.

For static performance, the final trimmed state of the aircraft is of interest. This trimming condition introduces an additional degree-of-freedom, namely the angle of incidence α, which is augmented to the DOF vector. The required additional equation is the fact that in a trimmed condition, the lift force needs to equilibrate the aircraft weight,

$$L = \frac{W}{2} \tag{14}$$

where W is the aircraft weight. Note that the symmetry of lift is taken into consideration. The lift force is found by taking the component of the reaction forces at the wing root, denoted by $\mathbf{R}_0$, perpendicular to the flow velocity direction

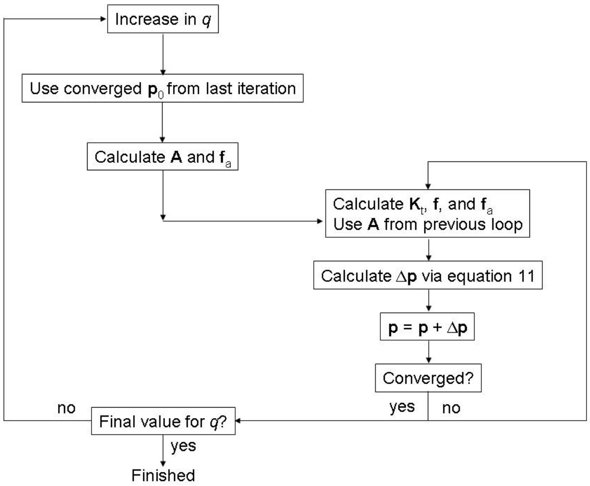

Figure 3: Overview of the two interlaced iteration loops

$\boldsymbol{\alpha}$ (see equation 6). Since the rotations and displacements at the root are required to be zero, the lift direction vector $\mathbf{e}_{l,0}$ is,

$$\mathbf{e}_{l,0} = [-\sin(\alpha) \;\; 0 \;\; \cos(\alpha)]^T \tag{15}$$

Thus the total lift and drag forces are given by,

$$L = \mathbf{R}_0^T \mathbf{e}_{l,0}, \quad D = \mathbf{R}_0^T \alpha. \tag{16}$$

The incremental equilibrium equation after augmenting the angle of incidence and the trim condition and removing the slave degrees of freedom takes the form,

$$\begin{bmatrix} \mathbf{J}(\mathbf{p}_0, q) & -\mathbf{f}_\alpha \\ \partial L/\partial q & \partial L/\partial \alpha \end{bmatrix} \Delta\mathbf{p} = \mathbf{f}_a(\mathbf{p}_0, q_{trim}) - \mathbf{f}(\mathbf{p}_0) + \mathbf{f}_w \tag{17}$$

where $\mathbf{f}_\alpha$ contains the sensitivities of the aerodynamic forces with respect to the angle of incidence α, and $\mathbf{f}_w$ represents the force induced by weight.

5. Morphing Wing Optimisation

The objective of the optimisation is to minimise the drag-to-lift ratio. The objective function $\mathcal{F}$ can hence be expressed as:

$$\mathcal{F} = \frac{D}{L}. \tag{18}$$

The design variables **b** are the rotation differences between the *master* and *slave* nodes. Hence, there are three design variables per physical node finite element. The hinge rotations are restrained by linear inequalities. The twisting angles are not allowed to exceed prescribed values for physical or geometric reasons such as for instance limitations on the sweep angle because of the presence of a tail. Furthermore limitations can be imposed on the actuator energy required for an angle change. The amount of energy needed should not be larger than the energy an off-the-shelf actuator can deliver.

The optimisation is carried out using Matlab®. The nonlinear gradient based constrained routine *fmincon* is used. Sensitivity information are obtained analytically using the direct method.[22]

6. Results

As an example an Uninhabited Aerial Vehicle (UAV) is used as a test case to show the abilities of the optimisation procedure. The UAV has a wing span of 16.6 *m*, a full-payload weight of 1,200 *kg*, a cruise speed of 50 m/s, a cruise altitude of 6,000 *m*. The wing chord is estimated to be 1.6 *m*. These dimensions are based on the Eagle-1 of the European Aeronautic Defence and Space Company (EADS).[23] At cruise speed at the cruising altitude, a lift-to-drag ratio of 10.64 at an angle-of-attack of 10.70 *deg* in trimmed condition was calculated. Since the wing is optimised for the cruise condition, it is the aim of the optimisation routine to re-optimise the wing shape in off-design conditions. Therefore it is investigated what the optimal wing configuration would be if the cruise speed is increased to 80 m/s.

It number of structural and aerodynamic panels used to discretise the whole wing is 10. The wing sweeping angle is restricted such that the sum of the nodal sweeping rotations do not exceed $\pm\ \pi/2$ in order to avoid collision with the Eagle's tail and to prevent the wing from sweeping into its own wake, since the aerodynamic model cannot account for that. Furthermore the folding angles per node are constrained to ± 1.0 *rad*, which should give enough optimisation freedom in that direction. Finally the wing twisting angle is restricted to ± 0.1 *rad* in order to limit the design space to physically meaningful twisting angles.

In the off-design condition, the lift-to-drag ratio drops to 7.83 and the trimmed angle-of-attack to 4.24 *deg*. It took the optimiser 36 iterations to find an optimal solution for the off-design flight condition. The optimised shape can be inspected in figure 4.

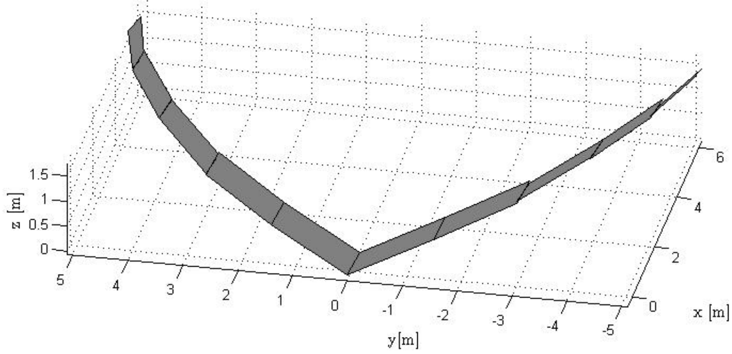

Figure 4: Optimised morphing wing shape

It is shown that the wing is folding, sweeping and twisting. The actual distribution is given in figure 5. The hinges indicated in the graphs are numbered from the root to the tip of the wing. It can be seen that the wing is folded upwards at the root to about 0.45 *rad* and then gradually folded back by an amount of -0.10 *rad* per hinge. The wing is twisted upwards near the tip to 0.04 *rad*, and twisted back to the neutral position at the next hinge. Then it remains constant until the last station, where the wing is twisted upwards to approximately 0.07 *rad*. Finally the wing has an almost continuous sweep back distribution of -0.27 *rad*.

The lift-to-drag ratio is increased by this morphing manoeuvre to 9.12, which is a 16 % improvement with respect to the original configuration.

7. Summary and Conclusions

In this paper an aeroelastic code for morphing wing analysis embedded in an optimisation routine is presented. The program incorporates a structural beam element code in a co-rotational framework coupled to a lifting-line aerodynamic model via a Newton-Raphson iteration method. It also allows morphing in any arbitrary direction in a three-dimensional space as well as the evaluation of the morphing energy associated with the morphing manoeuvre. The morphing wing was optimised for maximum lift-to-drag ratio in off-design conditions. It was demonstrated that by morphing a wing in the three-dimensional space, a substantial improvement in lift-to-drag ratio can be achieved. For the test case under consideration, it is demonstrated that three-dimensional morphing can improve aerodynamic performance substantially.

Future work will include the evaluation of the morphing energy to carry out the morphing manoeuvre and well as other optimisation criteria, such as flight mechanics. The optimisation routine will be updated such that the optimisation results in a feasible design. More real life UAV test cases will be investigated and design requirement will be postulated.

8. Acknowledgements

The authors would like to warmly acknowledge the contribution of Dr. Battini for putting his Matlab® code for the co-rotational framework at disposal. Furthermore Dr. Forth is acknowledged cordially for the use of his Matlab® toolbox on Automatic Differentiation. Finally the authors would like to thank Dr. Sanders and Mr. Reich of the AFRL for their valuable contribution and suggestions.

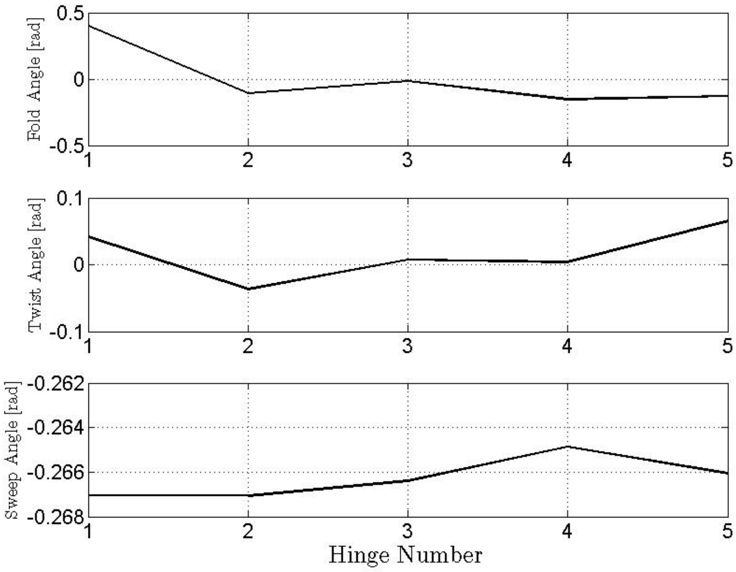

Figure 5: Morphing angle distribution

References

[1] Wilson, J.R. Morphing UAVs change the shape of warfare. In Aerospace America, February 2004.

[2] Gern, F.H. and Inman, D.J. and Kapania, R.K. Structural and Aeroelastic Modeling of General Planform Wings with Morphing Airfoils. In *AIAA Journal* 40(2):628-637, 2002.

[3] Gern, F.H. and Inman, D.J. and Kapania, R.K. Computation of Actuation Power Requirements for Smart Wings with Morphing Airfoils. In *Proceedings of the 43rd AIAA/ASME/ASCE/AHS/ASC Structures, Structural Dynamics and Materials Conference*, April 2002.

[4] Gern, F.H. and Inman, D.J. and Kapania, R.K. Computation of Actuation Power Requirements for Smart Wings with Mophing Airfoils. In *AIAA Journal* 43(12), 2005.

[5] Bae, J-S and Seigler, T.M. and Inman, D.J. Aerodynamic and Aeroelastic Considerations of a Variable-Span Morphing Wing. In *Proceedings of the 45th AIAA/ASME/ASCE/AHS/ASC Structures, Structural Dynamics and Materials Conference*, April 2004.

[6] De Breuker, R., Abdalla, M.M., Gürdal, Z. and Lindner, D. Energy-based Aeroelastic Analysis of a Morphing Wing. In *Proceedings of the Modeling, Signal Processing, and Control for Smart Structures*, April 2007.

[7] Prock, B.C. and Weisshaar, T.A. and Crossley, W.A. Morphing Airfoil Shape Change Optimization with Minimum Actuator Energy as an Objective, emphProceedings of the 9th AIAA/ISSMO Symposium of Multidisciplinary Analysis and Optimization, September 2002.

[8] Vale, J. and Lau, F. and Suleman, A. and Gamboa, P. Multidisciplinary Design Optimization of a Morphing Wing for and Experimental UAV, in *Proceedings of the 11th AIAA/ISSMO Multidisciplinary Analysis and Optimization Conference*, September 2006.

[9] Ricci, S. and Terraneo, M. Application of MDO Techniques to the Preliminary Design of Morphed Aircraft, *Proceedings of the 11th AIAA/ISSMO Multidisciplinary Analysis and Optimization Conference*, September 2006.

[10] Khot, N.S. and Zweber, J.V. and Veley, D.E. and Appa, K. and Eastep, F.E. Optimization of a Flexible Composite Wing for Pull-Up Maneuver with Internal Actuation. In *Proceedings of the 42nd AIAA/ASME/AHS/ASC Structures, Structural Dynamics and Materials Conference*, April 2001.

[11] Cook, A.M. and Crossley, W.A. Investigation of Genetic Algorithm Approaches for Smart Actuator Placement for Aircraft Maneuvering. In *Proceedings of the 39th AIAA Aerospace Sciences Meeting and Exhibit*, January 2001.

[12] Henderson, J.A. Global Optimisation Methods for Aeroservoelastic Concepts. In *Proceedings of the 43rd AIAA/ASME/AHS/ASC Structures, Structural Dynamics and Materials Conference*, April 2002.

[13] Gano, S.E. and Perez, V.M. and Renaud, J.E. and Batill, S.M. and Sanders, B. Multilevel Variable Fidelity Optimization of a Morphing Unmanned Aerial Vehicle. In *Proceedings of the 45th AIAA/ASME/AHS/ASC Structures, Structural Dynamics and Materials Conference*, April 2002.

[14] Goyal, V.K. and Kapania, R.K. A Shear-Flexible Beam Element for Linear Analysis of Unsymmetrically Laminated Beams. In *Proceedings of the 43rd AIAA/ASME/ASCE/AHS/ASC Conference*, April 2002.

[15] Cesnik, C.E.S. and Hodges, D.H. VABS: A New Concept for Composite Rotor Blade Cross-Sectional Modeling. In *Journal of the American Helicopter Society* 42(1):27-38, 1997.

[16] Battini, J-M and Pacoste, C. Co-rotational Beam Elements with Warping Effects in Instability Problems. In *Computer Methods in Applied Mechanics and Engineering* 191:1755-1789, 2002.

[17] Drela, M. Integrated Simulation Model for Preliminary Aerodynamic, Structural and Control-Law Design of Aircraft. In *Proceedings of the 40th AIAA/ASME/ASCE/AHS/ASC Structures, Structural Dynamics and Materials Conference*, April 1999.

[18] Abdulrahim, M. and Lind, R. Using Avian Morphology to Enhance Aircraft Maneuvrability. In *Proceedings of the AIAA Atmospheric Flight Mechanics Conference and Exhibit*, August 2006.

[19] Katz, J. and Plotkin, A. Low-Speed Aerodynamics, Second Edition. Cambridge University Press, 2001.

[20] Forth, S. and Edvall, M.M. User Guide for Mad - a Matlab Automatic Differentiation Toolbox TOMLAB/MAD. November 2006.

[21] Crisfield, M.A. Non-linear Finite Element Analysis of Solids and Structures. John Wiley & Sons Ltd., 1991.

[22] Haftka, R.T. and Gürdal, Z., Elements of Structural Optimization. Kluwer Academic, 1992.

[23] Okrent, M. Civil UAV Activity within the Framework of European Commission Research. In *AIAA 3rd Unmanned Unlimited Technical Conference, Workshop and Exhibit*, September 2004.

This page has been purposedly left blank